Electronic Supplementary Material (ESI) for Journal of Materials Chemistry C.

On the stability of calcium and cadmium based Ruddlesden-Popper and double perovskite structures

M. L. Marcondes, S. S. M. Santos, I. P. Miranda, P. Rocha-Rodrigues, L. V. C. Assali, A. M. L. Lopes, J. P. Araújo, and H. M. Petrilli

Electronic Supplementary information

Here we present supplementary information on the stability properties of the Ruddlesden-Popper (RP) $A_{n+1}B_nO_{3n+1}$ with $n = 1$ (RP1) and $n = 2$ (RP2) and double perovskite (DP) $AA'B_2O_6$ structures, where A, A′ = Ca, Cd and B = Mn, Ti.

Computational details

We used the generalized gradient approximation of Perdew-Burke-Ernzerhof (GGA-PBE) for the exchange-correlation functional, and expanded the wave functions within the projector augmented wave (PAW) method. We considered a cutoff energy of 110 Ry for the plane wave basis set and sampled the Brillouin zones (BZ) with an $8\times4\times4$ **k**-mesh, following the Monkhorst-Pack scheme. Previous theoretical studies have shown that spin-orbit coupling (SOC) might be important for ferroelectric properties. However, SOC has only minor effects in the systems studied here, causing slight deviations in the total energy but not affecting our main conclusions.

Supporting Information

Table S1 shows the equation of state parameters of the single perovskites, rock-salt oxides, and BO_2 systems used to compute the relative enthalpy for each crystalline component present in the possible dissociation chemical reaction, proposed in the Methodology section.

Table S1 Equation of state parameters for the single perovskites, rock-salt oxides, and BO_2 systems used to compute the phase stability properties. SG is the ground state space group, V_0 is the equilibrium volume (Å^3), K_0 the bulk modulus (GPa), and K_0' the bulk modulus pressure derivative (dimensionless).

System	SG	SG (#)	V_0	K_0	K_0'
$CaMnO_3$	$Pn'ma'$	62.448	211.06	176.7	4.38
$CaTiO_3$	$Pnma$	62	228.68	172.1	4.13
$CdMnO_3$	$R\bar{3}'$	148.19	211.03	188.1	4.59
$CdTiO_3$	$R\bar{3}$	148	226.55	186.5	4.37
CaO	$Fm\bar{3}m$	225	28.19	105.3	4.33
CdO	$Fm\bar{3}m$	225	27.22	123.9	4.71
MnO_2	$P4_2'/mnm'$	136.499	56.66	225.4	4.51
TiO_2	$P4_2/mnm$	136	64.28	202.9	4.91

Figure S1 shows the equations of state of the calcium and cadmium based RP2 and DP structures, up to 15 GPa.

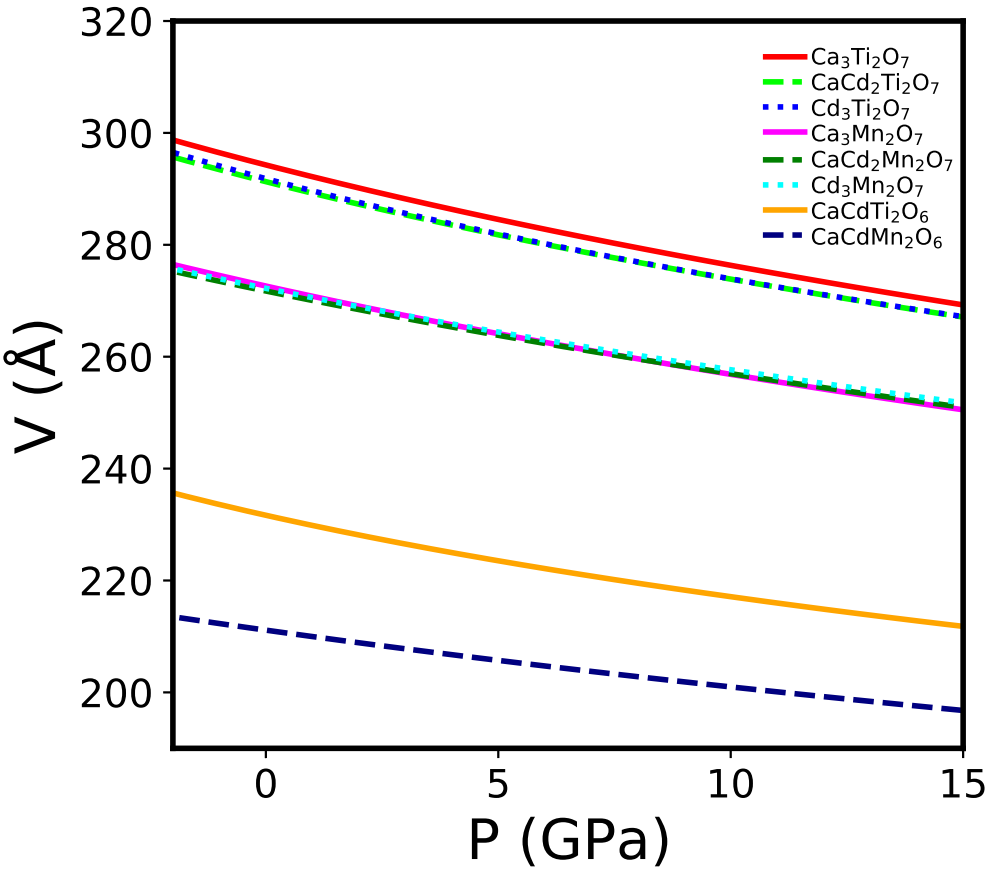

Figure S1 Equations of state (V × P) for the RP2 and DP structures based on Ca and Cd.

Figure S2 shows the relative enthalpy as a function of pressure for the RP2 structures.

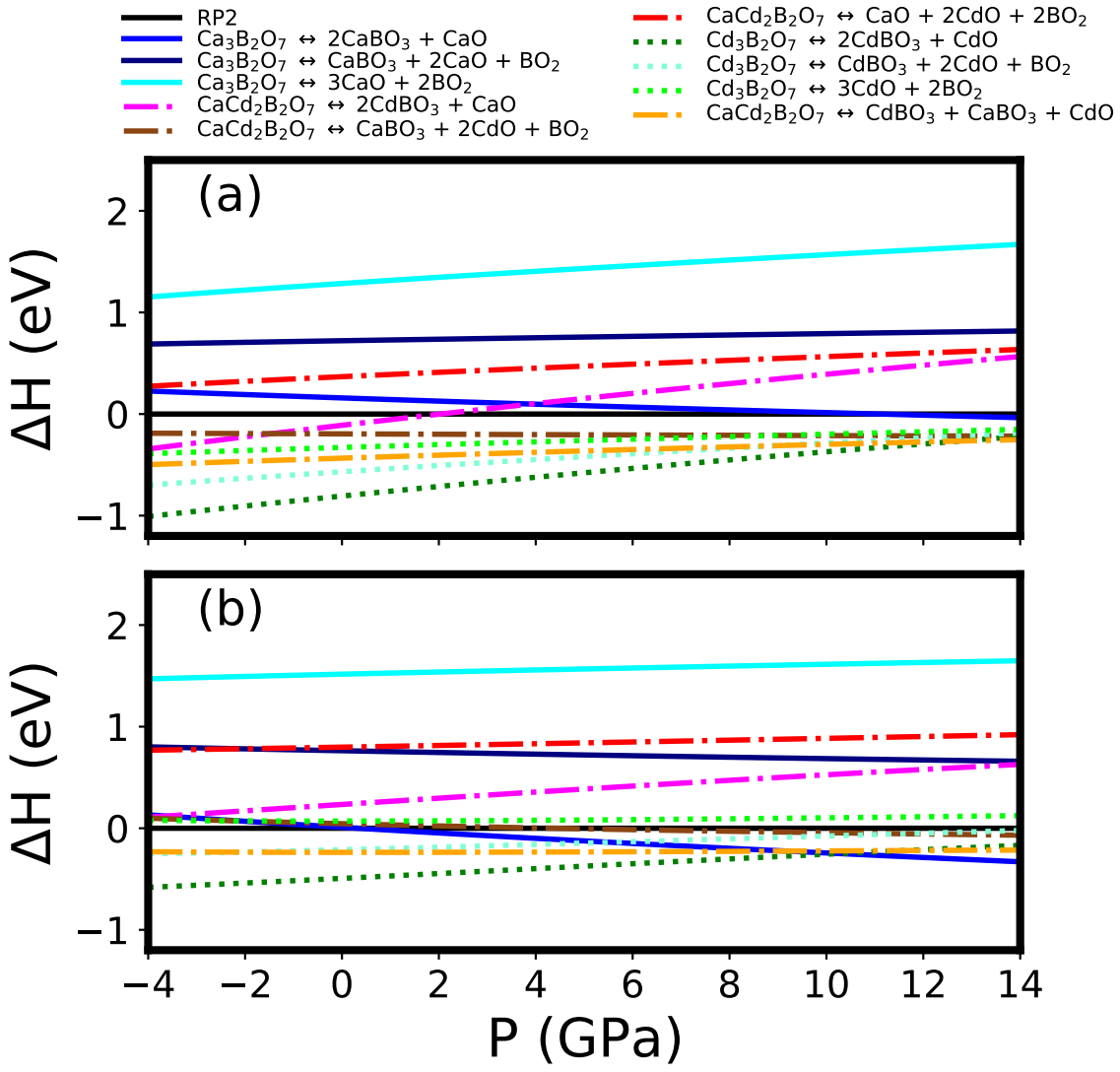

Figure S2 RP2 relative enthalpy ΔH, per f.u., as a function of pressure, for the dissociation reactions, w.r.t. the ground state $A2_1am$ phase, represented by the solid black lines at 0 eV. (a) B = Mn; (b) B = Ti.

Figure S3 compares the fitting model to compute the maximum Cd concentration x, at which the structure is still stable, for the $Ca_{3(1-x)}Cd_{3x}Ti_2O_7$ compound, with the *ab initio* calculations results. To obtain these data, we replaced Ca by Cd in all possible positions of the $Ca_3Ti_2O_7$ primitive cell, and computed the enthalpy for the lower energy configuration. There is a good agreement between the fitted line (blue) and the computed points. The orange line represents a fit of the *ab initio* results and the Cd concentration stability limit remains the same as the one found through the fitting model.

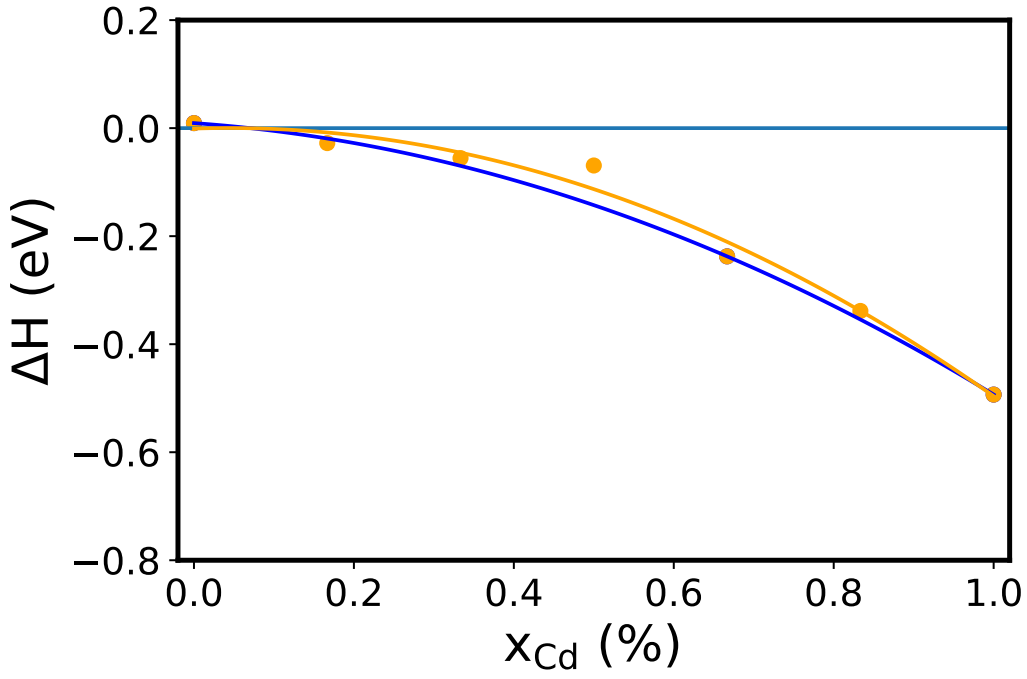

Figure S3 Comparison between our fitting model (blue line) and *ab initio* calculation results (orange dots) for several Cd concentrations in $Ca_{3(1-x)}Cd_{3x}Ti_2O_7$ primitive cell.

Figure S4 shows the equations of states of the A_2BO_4 compounds, where A = Ca, Cd and B = Mn, Ti. The crystal volumes are larger for the forsterite (*Pnma*) phase than for the RP1 (*Acam*) structure.

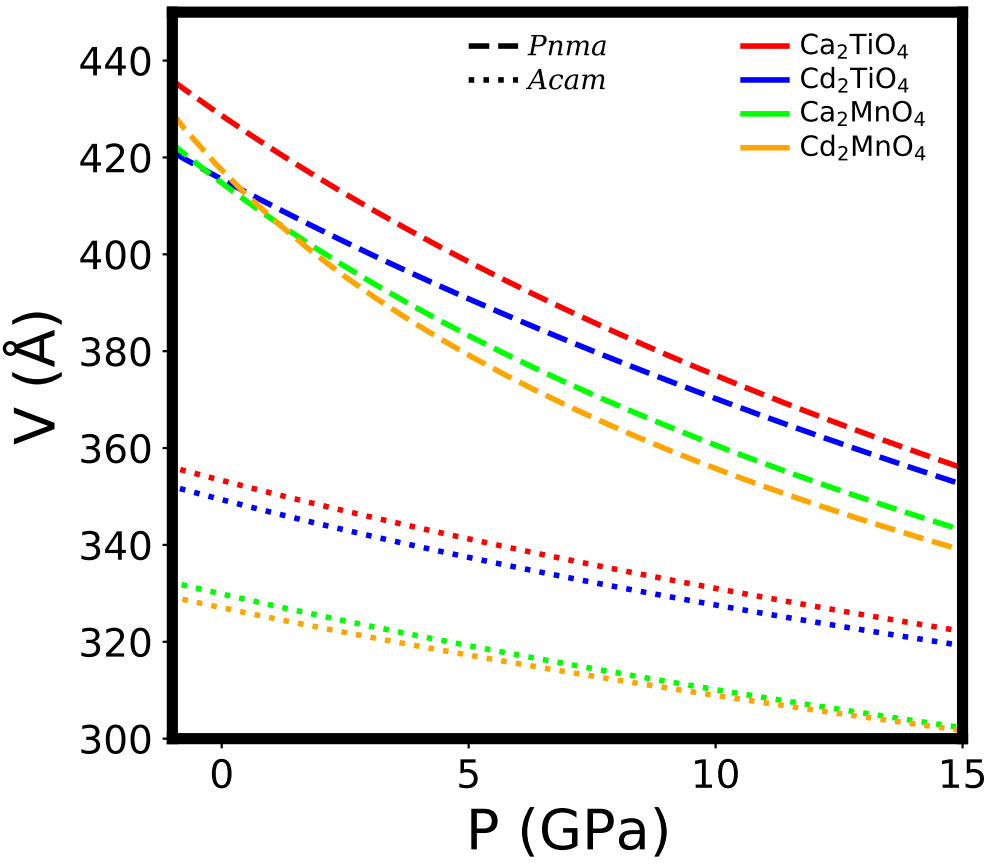

Figure S4 Equations of state (V × P) for the A_2BO_4 systems in the forsterite (*Pnma*) and in the RP1 (*Acam*) crystal structures.

Table S2 present the structural data of the Ca_2TiO_4 compound in the *Pnma* space group (forsterite phase).

Table S2 Crystal structure data of Ca_2TiO_4 in the *Pnma* space group (forsterite phase).

Lattice parameters (Å)				
a	11.48244			
b	6.81298			
c	5.42393			
Atomic positions				
Atom	Wyckoff	*x*	*y*	*z*
Ca1	4a	0.00000	0.00000	0.00000
Ca2	4c	0.77763	0.25000	0.49371
Ti	4c	0.59542	0.25000	0.93479
O1	4c	0.59280	0.25000	0.27560
O2	4c	0.95174	0.25000	0.71607
O3	8d	0.66271	0.03960	0.78105

Fig. S5 shows the calculated ground-state band structure and projected density of states (PDOS) of Ca_2TiO_4 compound, in the *Pnma* space group (forsterite), at null pressure. This material is an indirect band gap insulator (transition between M and Γ high symmetry points) with a gap energy of 4.23 eV. The top of the valence band is primarily composed by oxygen p states, while the bottom of the conduction band has its major contribution from titanium d states.

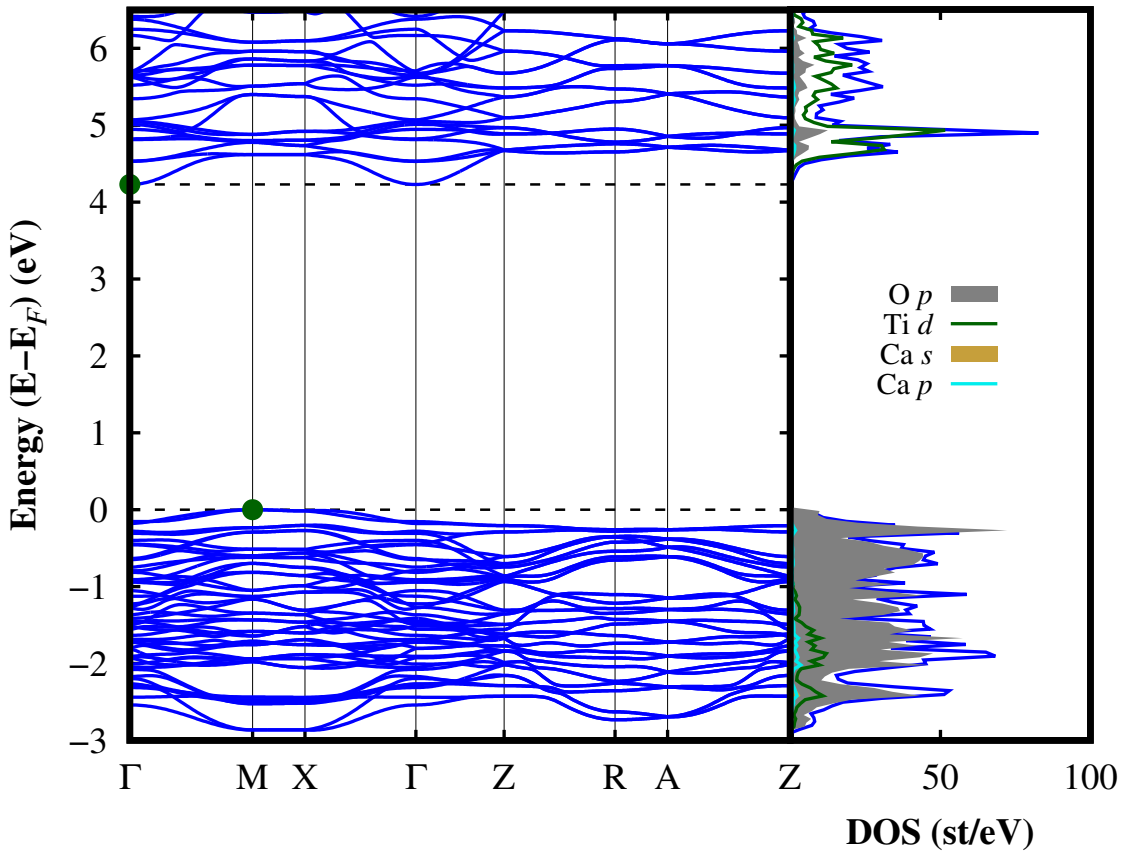

Figure S5 Electronic band structure and projected density of states of Ca_2TiO_4 in the forsterite structure, at null pressure. E_F is the Fermi energy.

Figure S6 displays the phonon dispersion curves of Cd_2TiO_4 compound in the *Pnma* space group. The phonon instabilities at the G (Γ), S, X, and Y first Brillouin zone (BZ) symmetry points indicate that the system is not dynamically stable.

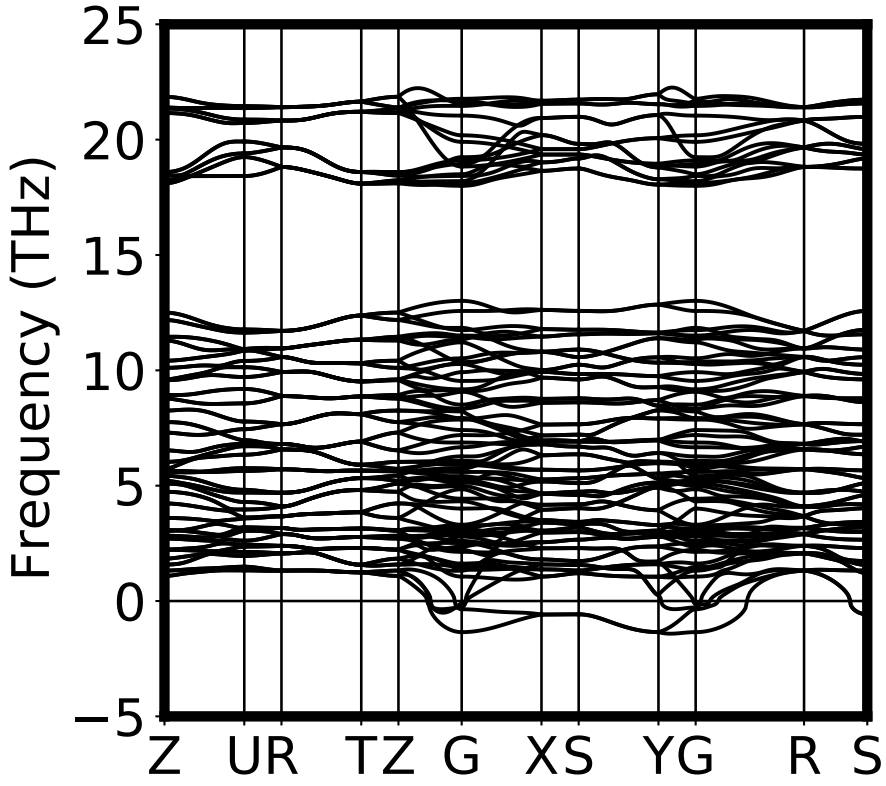

Figure S6 Phonon dispersion spectrum of the Cd_2TiO_4 along the main high-symmetry directions of the first BZ.

Figure S7 shows the phonon disperion of Ca_2TiO_4, demonstrating the dynamical stability of this system.

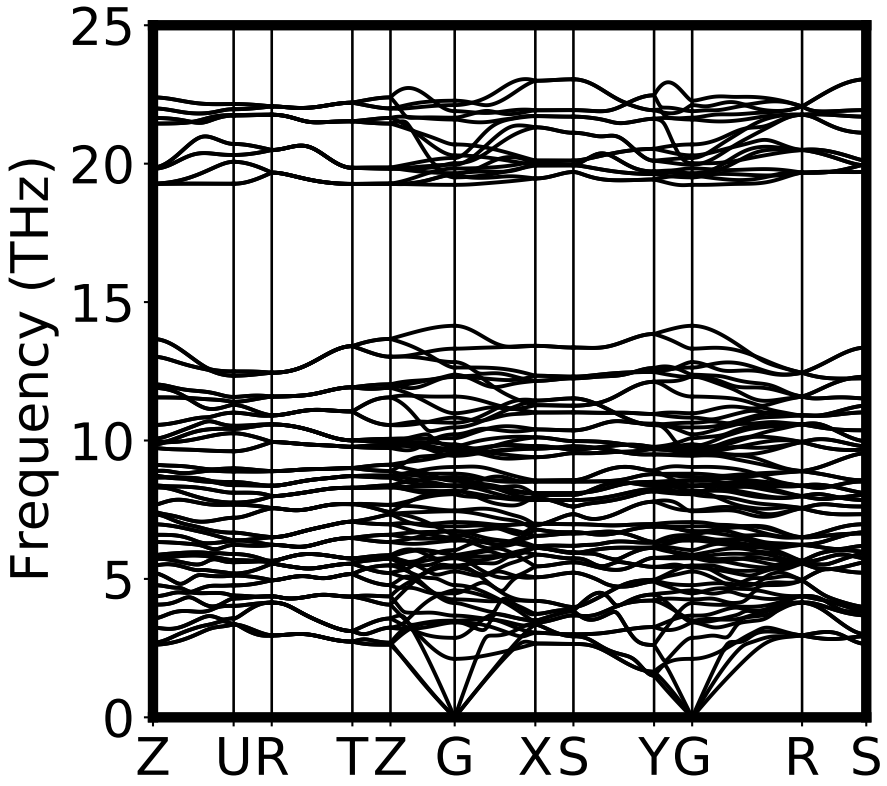

Figure S7 Phonon dispersion spectrum of the Ca_2TiO_4 in the *Pnma* space group (forsterite structure), along the main high-symmetry directions of the first BZ.

Figure S8 shows the relative enthalpy for the ABO_3 single perovskites, with A = Ca, Cd and B = Ti, Mn. For Cd-based systems the reference ground state belongs to the $R\bar{3}$ space group while for the Ca-based systems the reference ground state belongs to the *Pnma* space group. The dissociation chemical reactions are $ABO_3 \longleftrightarrow AO + BO_2$.

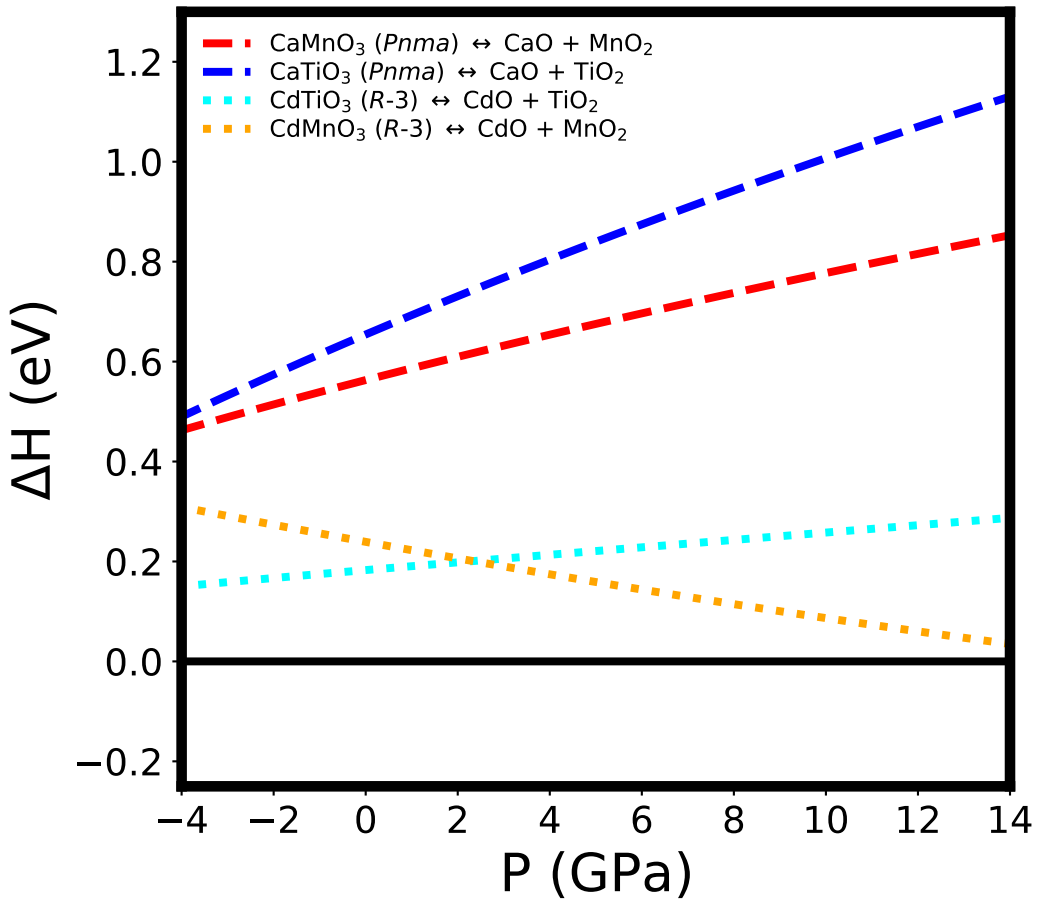

Figure S8 Phase stability of the $CaBO_3$ and $CdBO_3$ single perovskites (B = Mn, Ti).

Figure S9 shows the phonon disperion spectrum of $CaCdTi_2O_6$ at null pressure, demonstrating the dynamical stability of the system.

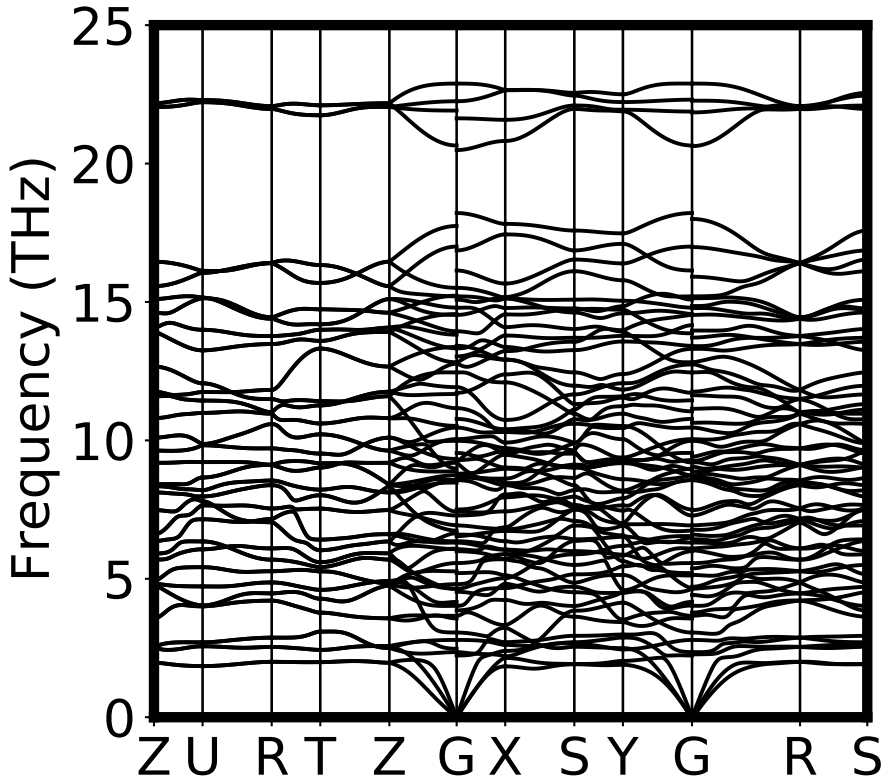

Figure S9 Phonon dispersion spectrum at 0 GPa of $CaCdTi_2O_6$ in the $Pmc2_1$ space group, along the main high-symmetry directions of the BZ.

Table S3 presents the structural data of the DP $CaCdTi_2O_6$ system in the $Pmc2_1$ space group.

Table S3 Crystal structure data of the DP $CaCdTi_2O_6$ compound in the $Pmc2_1$ space group.

Lattice parameters (Å)				
a		7.67669		
b		5.39706		
c		5.54506		
Atomic positions				
Atom	Wyckoff	x	y	z
Ca	2a	0.00000	0.26009	0.55269
Cd	2b	0.50000	0.75041	0.97057
Ti	4c	0.75142	0.24732	0.01975
O1	2a	0.00000	0.16796	0.97124
O2	2b	0.50000	0.66307	0.52118
O3	4c	0.79864	0.54631	0.78119
O4	4c	0.28957	0.05267	0.68484